Brazilian Journal of Physics (2021) 51:231–237
https://doi.org/10.1007/s13538-020-00849-5

SOCIEDADE BRASILEIRA DE FÍSICA

ATOMIC PHYSICS

Few-Neutron Systems with the Long-Range Casimir-Polder Force

R. Higa[1] · J. F. Babb[2]

Received: 6 October 2020 / Accepted: 14 December 2020 / Published online: 10 February 2021

Abstract
In this work, we present results of the long-range electromagnetic Casimir-Polder interactions between two neutrons, a neutron and a conducting wall, and a neutron between two walls. As input, we use the dynamic dipole polarizabilities of the neutron fitted to chiral EFT results up to the pion production threshold and at the onset of the Delta resonance. Our work can be relevant to the physics of confined ultracold neutrons inside bottles.

Keywords Casimir-Polder forces · Effective field theory · Ultracold neutrons

1 Introduction

The Casimir effect is a remarkable example of a phenomenon under deep contemplative analysis permeating through many different branches of physics [1–4]. It is often cited to illustrate the non-trivial concept of zero-point energy, or quantum fluctuations, giving rise to an observable force between two neutral objects. In its simplest version, the attractive force between two parallel, conducting plates is often recalled to explain the consequences of quantization of oscillating modes, at the heart of quantum physics, and the puzzling appearances of infinities that plague quantum field theories. Not only a necessity to explain certain quantum phenomena such as the behavior of specific heat of solids or the reduction of X-ray scattering from crystals at ultra-low temperatures [5], vacuum quantum fluctuations sustain the mystery of their contribution to the cosmological constant, which differs between predictions and observations by many orders of magnitude [5].

The broader meaning of the Casimir effect has its origins in experiments in the 1940s by Overbeek at Phillips Laboratory on quartz powder in colloid suspension (see [5] and references therein). The observed asymptotic behavior of the interactions disagreed with the van der Waals $1/r^6$ predictions and led Casimir and Polder to explain the mismatch in terms of retardation effects due to the finite speed of light. Backed by an insight from Niels Bohr, Casimir rederived and reinterpreted the so-called Casimir-Polder ($1/r^7$) forces in terms of changes in the zero-point energy [6]. It is this latter interpretation that excites the curiosity and interest of scientists from many distinct specializations in physics.

In atomic and molecular physics, specifically, a considerable amount of work has been dedicated to this subject [7]. Here, the so-called Casimir-Polder (CP) potential [8] for the electromagnetic interactions at very large separations describes the effects of the finite speed of light in mutual virtual photon mediated interactions between polarizable systems [1, 9]. Feinberg and Sucher [10] rederived the CP force between two neutral spinless particles in terms of the exchange of two virtual photons. The sum of all possible frequencies of the two virtual photons, obtainable from quantum field theory, has the same zero-point energy interpretation envisaged by Casimir. The Compton scattering of (virtual) photons on the neutral particle constitutes the subamplitude for the two-photon exchange process and carries information on the particle substructure as discussed in the following section.

In the present work, we use the terminology van der Waals (vdW) potential and Casimir-Polder potential in the following sense—both vdW and CP potentials are "long-range" electromagnetic interactions. Conventionally, "vdW interactions" refer to instantaneous Coulomb interactions.

✉ R. Higa
higa@if.usp.br

J. F. Babb
jbabb@cfa.harvard.edu

[1] Instituto de Física, Universidade de São Paulo, R. do Matão 1371, 05508-090, São Paulo, Brazil

[2] ITAMP, Center for Astrophysics, Harvard & Smithsonian, MS 14, 60 Garden St., Cambridge, MA 02138, USA

Moreover, the CP potential has as its "small separation distance" limit the vdW potential, the CP potential is valid for arbitrarily increasing separations (larger than some minimum separation at which "short-range" interactions, such as electron exchange in, for example, atomic physics, become negligible).

At asymptotically large separations, the CP potentials approach simple expressions involving only $\hbar$, c, the individual static polarizabilities $\alpha(0)$, and an inverse power of the separation distance (e.g., the behavior $1/r^7$ mentioned above with all coefficients becomes $-23\hbar c\alpha^2(0)/(4\pi r^7)$). Such asymptotic CP potentials are known for two neutral polarizable systems [8, 10], a neutral system and a charged system [9, 11, 12], for an atom and a perfectly conducting wall [8], etc. Thus, as we set forth in an earlier paper [13], it is reasonable, following an *ansatz* similar to that used by Spruch and Kelsey [9] for atoms, to write down the CP potential between two neutrons, a neutron and a wall, or a neutron between two walls in terms of the frequency-dependent polarizabilities $\alpha(\omega)$, where ω is the photon frequency.

Arnold [14] was the first to calculate effects of the CP potential—using the asymptotic $1/r^7$ potential—between two neutrons in nucleon-nucleon scattering; however, at that time only the static, electric dipole polarizability data were available with nowadays outdated values. We extended Arnold's idea [13, 15] to include dynamic electric and magnetic dipole polarizabilities with updated information from low-energy chiral effective field theory analysis. We also performed calculations of the CP interaction between a neutron and a wall, and one neutron between two walls. In the following, we summarize our main results and present an outlook for future studies.

2 Neutron Dynamic Dipole Polarizabilities

Electromagnetic probes have been one of the most important tools to extract information about the structure of hadrons. In the low ($E \lesssim 200$ MeV) and intermediate ($0.2 \lesssim E \lesssim 1$ GeV) energy region, Compton scattering made significant contributions to our understanding about the structure of the nucleon [16]. The electromagnetic field of the photon that hits the nucleon induces a response that can be parametrized in terms of the generalized multipole polarizabilities [16, 17], the leading dipole ones being inputs to our neutron-neutron CP potential. While dynamic dipole polarizabilities of the proton have been intensively studied and obtained from experiments with satisfactory precision, in the neutron case, one has to rely on strong isospin symmetry and bound neutron effects for Compton scattering on the deuteron [18, 19] and ^{3}He [20], or on nuclear structure uncertainties on neutron scattering of a large Z nucleus such as Pb [21].

Chiral effective field theory (χEFT), the effective theory rooted in the chiral symmetry of the underlying quantum chromodynamics (QCD), has been established as a rigorous and reliable theoretical framework to extract information about nucleon polarizabilities in the low-energy regime [16, 22]. The most updated χEFT calculation of Lensky, McGovern, and Pascalutsa [23] takes into account recoil corrections in a Lorentz-covariant way, improves convergence close to the pion production threshold, and includes the Delta (Δ) resonance explicitly. Their predictions for the neutron dynamic electric (α_n) and magnetic (β_n) dipole polarizabilities for photon energies up to $\omega_\gamma = 300$ MeV are nearly the same (within theoretical errorbars) to the proton case, as expected from isospin symmetry. In the static limit, they have $\alpha_n(0) = 13.7 \pm 3.1$ and $\beta_n(0) = 4.6 \pm 2.7$, in units of 10^{-4} fm^3.

The relations between the dynamic dipole polarizabilities and either Compton scattering observables or theory predictions are quite involved [16]. Therefore, we provide a parametrization of $\alpha_n(\omega)$ and $\beta_n(\omega)$ that tries to incorporate the relevant low-energy physics with simple formulas. They take the form:

$$\alpha_n(\omega) = \frac{\alpha_n(0)\sqrt{(m_\pi+a_1)(2M_n+a_2)}(0.2a_2)^2}{\sqrt{(\sqrt{m_\pi^2-\omega^2}+a_1)(\sqrt{4M_n^2-\omega^2}+a_2)}\left[|\omega|^2+(0.2a_2)^2\right]}, \quad (1)$$

$$\beta_n(\omega) = \frac{\beta_n(0)-b_1^2\omega^2+b_2^3\,\mathrm{Re}(\omega)}{(\omega^2-\omega_\Delta^2)^2+|\omega^2\Gamma_\Delta^2|}, \quad (2)$$

with M_n the neutron mass, m_π the pion mass, and a set of adjustable parameters given in Table 1. The square roots in (1) emulate the non-analytic threshold behavior related to the photoproduction of a pion [22, 23] and (2) takes the form of an energy-dependent Breit-Wigner that incorporates the physics of the Δ resonance. Our parameters are fitted to the theoretical curves of Lensky et al. [23] in three different ways. In Set 1, we let $\alpha_n(0)$ and $\beta_n(0)$ be free parameters, in Set 2 we fix them to the PDG central value [24], and

Table 1 Parameters of (1), (2) fitted to the theoretical curves of Ref. [23]. $\alpha_n(0)$ and $\beta_n(0)$ units are 10^{-4}fm^3, the remaining ones in MeV

	$\alpha_n(0)$	a_1	a_2	$\beta_n(0)$	b_1	b_2	ω_Δ	Γ_Δ
Set 1	13.9968	12.2648	1621.63	4.2612	8.33572	22.85	241.484	66.92 65
Set 2	11.6	2.2707	2721.47	3.7	8.67962	24.2003	241.593	68.3009
Set 3	12.5	5.91153	2118.79	2.7	9.27719	26.328	241.821	70.8674

in Set 3 we fix them to the central value of Kossert et al. [25]. The quality of the parametrization can be seen in Fig. 1 and is satisfactory for our purposes, falling well within the theoretical error bars [23]. In particular, on the left panel one sees the cusp behavior associated to the pion photoproduction, and on the right panel, the increase of β_n near the delta-neutron mass difference ~ 230 MeV [13].

As shown in the following, the basic inputs to our CP interactions are the dynamic dipole polarizabilities α_n and β_n evaluated at imaginary frequencies. To make sure our (1) and (2) are reasonable in the complex domain, we make a numeric comparison of these parametrizations with the heavy-baryon chiral perturbation theory (HB-χPT) expressions of Hildebrandt et al., given in Appendices B and C of Ref. [26]. The latter are given by the thin solid lines in Fig. 1, for real photon energies. The same expressions were extended to imaginary energies, and we checked that agree with our parametrizations up to $i\omega \lesssim i\, m_\pi$ (see [13] for a detailed discussion).

3 Neutron Under Casimir-Polder Forces

In this section, we recollect the main formulas and results from our previous works [13, 15, 27]. We consider only the parameters from Set 1, which represents qualitatively the other sets.

The CP interaction between two neutrons is given by [7, 9, 10, 13]:

$$\begin{aligned} V_{CP,nn}(r) &= -\frac{\alpha_0}{\pi r^6}\, I_{nn}(r)\,, \\ I_{nn}(r) &= \int_0^\infty d\omega\, e^{-2\alpha_0\omega r} \Big\{ \Big[\alpha_n(i\omega)^2 + \beta_n(i\omega)^2\Big]\, P_E(\alpha_0\omega r) \\ &\quad + \left[\alpha_n(i\omega)\beta_n(i\omega) + \beta_n(i\omega)\alpha_n(i\omega)\right] P_M(\alpha_0\omega r) \Big\}\,, \\ P_E(x) &= x^4 + 2x^3 + 5x^2 + 6x + 3\,, \\ P_M(x) &= -(x^4 + 2x^3 + x^2)\,, \end{aligned} \tag{3}$$

where $\alpha_0 \approx 1/137$ is the electromagnetic fine structure constant. Due to the exponential factor $\exp(-2\alpha_0\omega r)$ in the above formula, it is straightforward to check that the asymptotic region $r \to \infty$ is dominated by frequencies $\omega \to 0$. In the static limit, the integral can be performed analytically and one arrives at the original Casimir-Polder result, $V^\star_{CP,nn}(r) = V_{CP,nn}(r \to \infty) = -\left[23(\alpha_n^2(0) + \beta_n^2(0)) - 14\alpha_n(0)\beta_n(0)\right]/(4\pi r^7)$. The static limit serves as a numerical check, though it happens at distances much larger than the hadronic/nuclear scale of a few fm, as we discuss in the following. As one moves inwards, the effects of frequency-dependent polarizabilities become apparent from low to high values of ω.

Figure 2 shows the behavior of the CP potential between two neutrons (dashed line), compared to the static limit (solid line). In the left panel, one sees a quenching in the strength of the interaction due to the dependence on the frequency of the polarizabilities. The right panel allows one to quantify better the large distance behavior. The short-dashed curve is the CP potential multiplied by $s\, r^6$, where $s = 100$ fm to fit in the figure. The long-dashed and thick-solid curves stand for the dynamic ($V_{CP,nn}$) and static ($V^\star_{CP,nn}$) polarizabilities versions of the potential, respectively, multiplied by r^7. The thin solid curve is the arctan parametrization [28] that connects the $1/r^7$ asymptotic CP and the mid-distance $1/r^6$ vdW behaviors. One sees that at small distances $r \lesssim 20$ fm there is a clear $1/r^6$ behavior, meaning that the integrand of (3) is nearly constant. From the exponential factor, one concludes that this region is probing neutron excitations larger than $(2\alpha_0 \times 20\,\text{fm})^{-1} \sim 670$ MeV. The Δ resonance has its biggest influence around $(2\alpha_0\omega_\Delta)^{-1} \sim 50$ fm, though it contributes primarily to β_n, which is much smaller than the α_n contribution. The energy related to the pion production threshold affects distances around $(2\alpha_0\omega_\pi)^{-1} \sim 100$ fm.

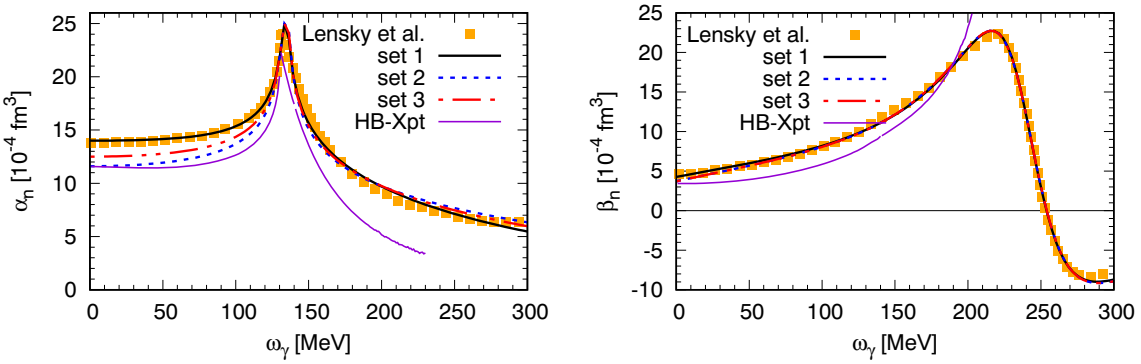

Fig. 1 Dynamic electric (left) and magnetic (right) polarizabilities, as functions of the photon energy ω_γ. The yellow squares are χEFT results of Lensky et al. [23], while sets 1, 2, and 3 correspond to our parametrizations using the numbers specified in Table 1. The thin solid lines are HB-χEFT results from Ref. [26]. Adapted from [13]

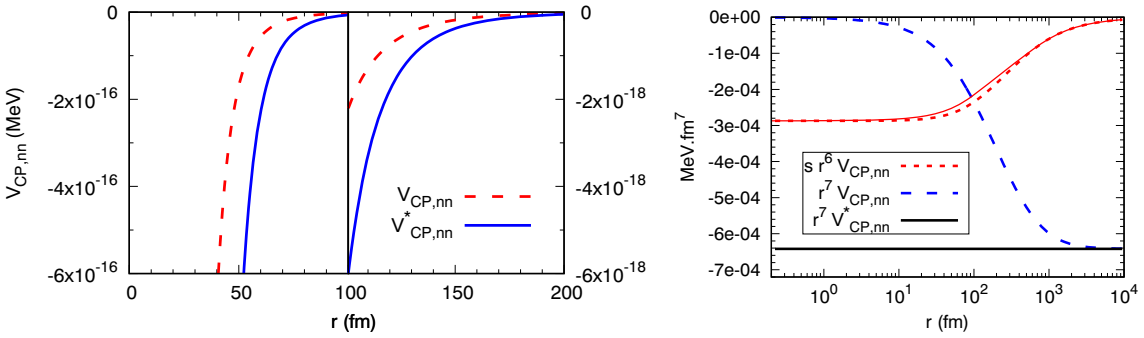

Fig. 2 Results for the CP interaction between two neutrons. Adapted from [13]

The asymptotic $1/r^7$ behavior is achieved only beyond 10^3 fm, due to dynamic polarizabilities with frequencies $\omega_\gamma \lesssim 10$ MeV.

For the neutron-Wall (nW) CP potential one has [13, 29, 30]

$$\begin{aligned} V_{CP,nW}(r) &= -\frac{\alpha_0}{4\pi r^3} J_{nW}(r)\,, \\ J_{nW}(r) &= \int_0^\infty d\omega\, e^{-2\alpha_0\omega r}\alpha_n(i\omega)Q(\alpha_0\omega r)\,, \\ Q(x) &= 2x^2+2x+1\,, \end{aligned} \tag{4}$$

where for this pilot study, we consider only the electric polarizability α_n component. (The magnetic polarizability term of the total nW CP potential enters with the opposite sign [31], though for the neutron $\alpha_n(0)/\beta_n(0) \sim 3$, so one might view (4) as the most optimistic estimate of the effect.) The asymptotic limit of (4) gives $V^\star_{CP,nW}(r) = V_{CP,nW}(r\to\infty) = -3\alpha_n(0)/(8\pi r^4)$.

Figure 3 shows the CP interaction between a neutron and a wall, as a function of the separation r. On the right panel, the short-dashed curve is multiplied by $s\,r^3$ with $s = 100$ fm. The long-dashed and thick-solid curves are analogous to the $V_{CP,nn}$ case, multiplied by r^4 instead. The qualitative features of the mid-distance $1/r^3$ and the asymptotic $1/r^4$ behaviors are practically the same as the $V_{CP,nn}$ case.

For two walls separated by a distance L and one neutron in between, at a distance z from the midpoint [13, 29, 30], the CP potential reads:

$$V_{CP,WnW}(z,L) = -\frac{1}{\alpha_0\pi L^4}\int_0^\infty u^3 du\,\alpha_n\left(i\frac{u}{\alpha_0 L}\right)\int_1^\infty \frac{dv}{\sinh(uv)}\left[v^2\cosh\left(\frac{2z}{L}uv\right)-e^{-uv}\right]. \tag{5}$$

In the static limit, the integral can be done analytically and leads to:

$$\begin{aligned} V^\star_{CP,WnW}(z,L) &= -\frac{\alpha_n(0)}{\alpha_0\pi L^4}\left\{\frac{3}{8}\left[\zeta\left(4,\frac{1-f}{2}\right)\right.\right. \\ &\quad \left.\left.+\zeta\left(4,\frac{1-f}{2}\right)\right]-\frac{\zeta(4,1)}{4}\right\} \\ &= -\frac{\pi^3\alpha_n(0)}{\alpha_0 L^4}\left[\frac{3-2\cos^2(\pi f/2)}{8\cos^4(\pi f/2)}-\frac{1}{360}\right], \end{aligned} \tag{6}$$

where $f = 2z/L$ and

$$\zeta(a,b) = \sum_{k=0}^{\infty}\frac{1}{(k+b)^a} \tag{7}$$

is the generalized Zeta function. Equation (6) explicitly shows the asymptotic L^{-4} behavior of $V_{CP,WnW}$.

Figure 4 shows the CP interaction of a neutron between two walls. The right panel shows its dependence of $V_{CP,WnW}$ on both L and z while on the left panel one has the z dependence of both $V_{CP,WnW}$ (dashed line) and $V^\star_{CP,WnW}$ (solid line), for three selected values of L.

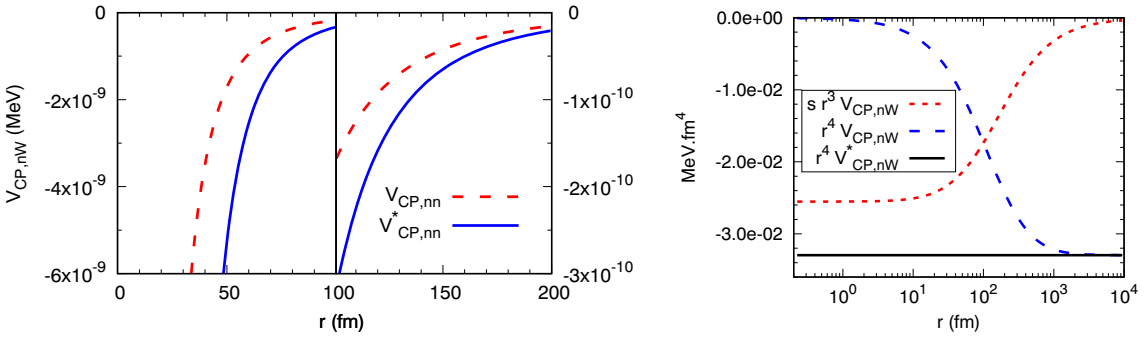

Fig. 3 Results for the CP interaction between a neutron and a wall. Adapted from [13]

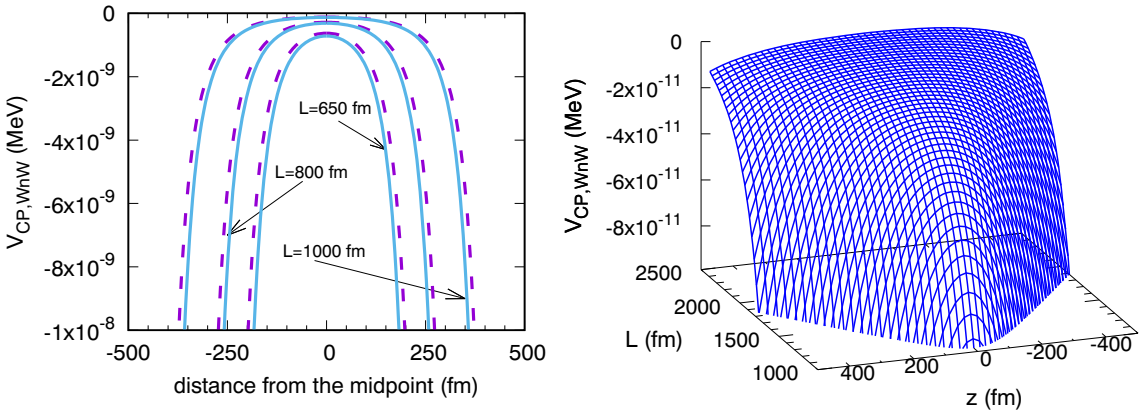

Fig. 4 Results for the CP interaction of a neutron between two walls, as a function of the neutron distance from the midpoint z. Adapted from [13]

4 Discussions and Concluding Remarks

In this work, we extend to neutron physics the phenomenology of the CP forces developed in atomic and molecular physics. We present the CP interactions between two neutrons, a neutron and a wall, and a neutron between two walls. This work goes beyond the static limit, taking into consideration the frequency dependence of the electric and magnetic dipole polarizabilities of the neutron. It embraces the same spirit as the work by Spruch and Kelsey [9] regarding dynamic polarizabilities.

One finds that the CP interactions between two neutrons and between a neutron and a wall have their long-distance behavior driven by the low-energy dynamics of the Compton sub-amplitude. Chiral dynamics provides reliable predictions for Compton scattering observables up to around the excitation energy of the Δ resonance, $\sim$ 300 MeV. Therefore, our results are not reliable for distances shorter than $\sim$ 30 fm. The low-energy dynamics associated with the Δ resonance and the one-pion photoproduction dictate the behavior of the CP interactions around 50 fm and 100 fm, respectively. One observes the smooth transition from the vdW-like to the asymptotic CP-like behavior over a range as large as $r \sim 10^3$ fm, though only beyond such distances do our CP interactions reach the expected static limit.

In the asymptotic $1/r^7$ regime, the value of the neutron-neutron CP potential may be too small to be of any relevance to hadronic/nuclear physics. However, in the physics of ultracold neutrons, the slower $1/r^4$ tail of the neutron-wall and the wall-neutron-wall CP potentials may compete with other important effects. For instance, the repulsive Fermi pseudo-potential energies close to the surface of nickel and aluminium are about 252 neV and 54 neV, respectively [13]. This is comparable to the value of the neutron-wall CP interaction at $r \sim 1500$ fm. Clearly, a more quantitative estimate of these effects ought to be carried out by experiments aiming at confinement of ultracold neutrons. For instance, our (4) and (5) take into account only the electric dynamic dipole polarizability. Contributions from the magnetic polarizability were addressed in the static limit in [31] and are expected to be non-negligible. Besides, at this length scale, the perfect conducting wall approximation used here as in atomic physics does not model effects due to the spatial extension of atoms and their arrangement in a real metal condition; these and other considerations might be especially important for neutron distances very close to the wall.

Other possible places where CP interactions may have some relevance are in systems with three and four neutrons [15]. The existence of bound, virtual, or resonant states in these systems is an old and persistent question in few-body nuclear physics. While bound states are quite improbable due to constraints of the nuclear interactions fitted to other nuclei, the existence of three or four neutron resonances remains a controversial topic [32–36], especially due to a recent observation of a signal compatible with a four-neutron resonance [37]. Without dealing with the nuclear interaction part which can be quite involved, one asks if a long-range electromagnetic interaction such as the CP force is able to change the position or either the nature of the possible three- and four-neutron states. The potential energy due to the CP force was estimated in [15] for two different configurations of three neutrons, and one for four neutrons. An equilateral triangle arrangement of neutrons with sides of length r gives a repulsion of $\sim 1.73\,\hbar c\alpha_n^3/(\pi r^{10})$ and a linear chain of three neutrons equally separated by $r/2$ gives an attraction of $\sim -186\,\hbar c\alpha_n^3/(\pi r^{10})$. Four neutrons in a tetrahedron configuration with edge length r lead to an attraction of $\sim -633\,\hbar c\alpha_n^4/(\pi r^{13})$.

Mahir was a frequent visitor to The Institute for Theoretical Atomic, Molecular, and Optical Physics (ITAMP), gave seminars in 1995, 1996, 2000, and 2011, and collaborated widely in active discussions with Institute staff and

postdoctoral fellows resulting in publications with Vasili Kharchenko, Robin Côté, Eddy Timmermans, Paolo Tommasini, and Jack Wells.

Our work on neutron and proton Casimir-Polder forces originated during Mahir's 2011 visit to ITAMP, during which he became aware of available *frequency-dependent* electric and magnetic dipole polarizabilities of n and p, complementing the well-known *static* polarizabilities. JFB learned of Mahir's earlier work (from 1990) proposing [38] a method to look for color (QCD) van der Waals forces [39, 40] that inspired an experiment [41] and Mahir believed that the time had come to take a fresh look at QED van der Waals forces among neutrons and protons. His intuition was correct—we found only the previous related study (discussed in Section 1) from 1973 [14].

Mahir's imagination and expertise in the quantum mechanics of atomic, nuclear, and molecular systems is evident in his many works, collaborations, and services to science. His respectability and leadership in the Brazilian nuclear physics community are attested by the formation of generations of nuclear scientists, his recognized scientific production and vision, and his pivotal role in promoting the construction of the rare isotope beam facility RIBRAS at the University of São Paulo. Mahir was truly an "ambassador of physics" and he will be greatly missed.

Funding Work supported in part by the Brazilian agency FAPESP thematic projects 2017/05660-0 and 2019/07767-1, and INCT-FNA Proc. No. 464898/2014-5 (RH), and the US NSF through a grant for ITAMP at Harvard University and the Smithsonian Astrophysical Observatory (JFB).

References

1. L. Spruch, Long-range (Casimir) interactions. Science **272**(5267), 1452 (1996). https://doi.org/10.1126/science.272.5267.1452
2. L. Spruch, A. Stange, D.K. Campbell, D.J. Bishop, Phys. Today **74**(1), 42 (2021). https://doi.org/10.1063/PT.3.4656
3. A.W. Rodriguez, P.C. Hui, D.P. Woolf, S.G. Johnson, M. Lončar, F. Capasso, Classical and fluctuation-induced electromagnetic interactions in micron-scale systems: designer bonding, antibonding, and Casimir forces. Annalen der Physik **527**(1-2), 45 (2015). https://doi.org/10.1002/andp.201400160
4. L.H. Ford, M.P. Hertzberg, J. Karouby, Quantum gravitational force between polarizable objects. Phys. Rev. Lett. **116**(15), 151301 (2016). https://doi.org/10.1103/PhysRevLett.116.151301
5. P.W. Milonni, M.L. Shih, Casimir forces. Contemp. Phys. **33**, 313 (1992). https://doi.org/10.1080/00107519208223981
6. H.B.G. Casimir, Sur les forces Van der Waals-London. J. Chim. Phys. **46**, 407 (1949). https://doi.org/10.1051/jcp/1949460407
7. J.F. Babb. in *Adv. At. Molec. Opt. Phys.*, ed. by E. Arimondo, P.R. Berman, C.C. Lin, Vol. 59 (Academic, San Diego, 2010), pp. 1–20, https://doi.org/10.1016/S1049-250X(10)59001-3
8. H.B.G. Casimir, D. Polder, The influence of retardation on the London-van der Waals forces. Phys. Rev. **73**, 360 (1948). https://doi.org/10.1103/PhysRev.73.360
9. L. Spruch, E.J. Kelsey, Vacuum fluctuation and retardation effects on long-range potentials. Phys. Rev. A **18**(3), 845 (1978). https://doi.org/10.1103/PhysRevA.18.845
10. G. Feinberg, J. Sucher, General theory of the van der Waals interaction: A model-independent approach. Phys. Rev. A **2**(6), 2395 (1970). https://doi.org/10.1103/PhysRevA.2.2395
11. J. Bernabéu, R. Tarrach, Long-range potentials and the electromagnetic polarizabilities. Ann. Phys. (N.Y.) **102**(1), 323 (1976). https://doi.org/10.1016/0003-4916(76)90265-7
12. G. Feinberg, J. Sucher, Long-range forces between a charged and neutral system. Phys. Rev. A **27**(4), 1958 (1983). https://doi.org/10.1103/PhysRevA.27.1958
13. J.F. Babb, R. Higa, M.S. Hussein, Dipole-dipole dispersion interactions between neutrons. Eur. Phys. J. A **53**(6), 126 (2017). https://doi.org/10.1140/epja/i2017-12313-7
14. L.G. Arnold, Neutron polarizability and the two-neutron scattering length. Phys. Lett. B **44**(5), 401 (1973). https://doi.org/10.1016/0370-2693(73)90318-3
15. M.S. Hussein, J.F. Babb, R. Higa, The Casimir-Polder interaction between two neutrons and possible relevance to tetraneutron states. Acta Phys. Pol. B **48**(10), 1837 (2017). https://doi.org/10.5506/APhysPolB.48.1837
16. F. Hagelstein, R. Miskimen, V. Pascalutsa, Nucleon polarizabilities: From Compton scattering to hydrogen atom. Prog. Part. Nucl. Phys. **88**, 29 (2016). https://doi.org/10.1016/j.ppnp.2015.12.001
17. I. Guiaşu, E. Radescu, Higher multipole polarizabilities of hadrons from compton scattering amplitudes. Ann. Phys. (N. Y.) **120**(1), 145 (1979). https://doi.org/10.1016/0003-4916(79)90285-9
18. M. Lundin, J.O. Adler, M. Boland, K. Fissum, T. Glebe, K. Hansen, L. Isaksson, O. Kaltschmidt, M. Karlsson, K. Kossert, M.I. Levchuk, P. Lilja, B. Lindner, A.I. L'vov, B. Nilsson, D.E. Oner, C. Poech, S. Proff, A. Sandell, B. Schröder, M. Schumacher, D.A. Sims, Compton scattering from the deuteron and extracted neutron polarizabilities. Phys. Rev. Lett. **90**, 192501 (2003). https://doi.org/10.1103/PhysRevLett.90.192501
19. L.S. Myers, J.R.M. Annand, J. Brudvik, G. Feldman, K.G. Fissum, H.W. Grießhammer, K. Hansen, S.S. Henshaw, L. Isaksson, R. Jebali, M.A. Kovash, M. Lundin, J.A. McGovern, D.G. Middleton, A.M. Nathan, D.R. Phillips, B. Schröder, S.C. Stave, Measurement of compton scattering from the deuteron and an improved extraction of the neutron electromagnetic polarizabilities. Phys. Rev. Lett. **113**, 262506 (2014). https://doi.org/10.1103/PhysRevLett.113.262506
20. J. Annand, B. Strandberg, H.J. Arends, A. Thomas, E. Downie, D. Hornidge, M. Morris, V. Sokoyan, Compton scattering from ^{3} he using an active target. PoS Proc. Sci. **CD15**, 092 (2016). https://doi.org/10.22323/1.253.0092
21. J. Schmiedmayer, P. Riehs, J.A. Harvey, N.W. Hill, Measurement of the electric polarizability of the neutron. Phys. Rev. Lett. **66**, 1015 (1991). https://doi.org/10.1103/PhysRevLett.66.1015
22. H. Griesshammer, J. McGovern, D. Phillips, G. Feldman, Using effective field theory to analyse low-energy Compton scattering data from protons and light nuclei. Prog. Part. Nucl. Phys. **67**, 841 (2012). https://doi.org/10.1016/j.ppnp.2012.04.003
23. V. Lensky, J.A. McGovern, V. Pascalutsa, Predictions of covariant chiral perturbation theory for nucleon polarisabilities and polarised Compton scattering. Eur. Phys. J. D **75**, 604 (2015). https://doi.org/10.1140/epjc/s10052-015-3791-0
24. C. Patrignani, et al., Review of particle physics. Chin. Phys. C **40**(10), 100001 (2016). https://doi.org/10.1088/1674-1137/40/10/100001
25. K. Kossert et al., Quasifree Compton scattering and the polarizabilities of the neutron. Eur. Phys. J. A **16**, 259 (2003). https://doi.org/10.1140/epja/i2002-10093-9

26. R.P. Hildebrandt, H.W. Griesshammer, T.R. Hemmert, B. Pasquini, Signatures of chiral dynamics in low-energy compton scattering off the nucleon. Eur. Phys. J. A **20**, 293 (2004). https://doi.org/10.1140/epja/i2003-10144-9
27. R. Higa, J.F. Babb, M.S. Hussein, Dipole-dipole interactions between neutrons. Springer Proc. Phys. **238**, 873 (2020). https://doi.org/10.1007/978-3-030-32357-8_137
28. M. O'Carroll, J. Sucher, Arctangent approximation to the intermolecular potential. Phys. Rev. **187**(1), 85 (1969). https://doi.org/10.1103/PhysRev.187.85
29. F. Zhou, L. Spruch, van der Waals and retardation (Casimir) interactions of an electron or an atom with multilayered walls. Phys. Rev. A **52**(1), 297 (1995). https://doi.org/10.1103/PhysRevA.52.297
30. Z.C. Yan, A. Dalgarno, J.F. Babb, Long-range interactions of lithium atoms. Phys. Rev. A **55**(4), 2882 (1997). https://doi.org/10.1103/PhysRevA.55.2882
31. T.H. Boyer, Recalculations of long-range van der Waals potentials. Phys. Rev. **180**(1), 19 (1969). https://doi.org/10.1103/PhysRev.180.19
32. A.M. Shirokov, G. Papadimitriou, A.I. Mazur, I.A. Mazur, R. Roth, J.P. Vary, Prediction for a four-neutron resonance. Phys. Rev. Lett. **117**, 182502 (2016). https://doi.org/10.1103/PhysRevLett.117.182502
33. S. Gandolfi, H.W. Hammer, P. Klos, J.E. Lynn, A. Schwenk, Is a trineutron resonance lower in energy than a tetraneutron resonance?. Phys. Rev. Lett. **118**, 232501 (2017). https://doi.org/10.1103/PhysRevLett.118.232501
34. K. Fossez, J. Rotureau, N. Michel, M. Płoszajczak, Can tetraneutron be a narrow resonance? Phys. Rev. Lett. **119**, 032501 (2017). https://doi.org/10.1103/PhysRevLett.119.032501
35. E. Hiyama, R. Lazauskas, J. Carbonell, M. Kamimura, Possibility of generating a 4-neutron resonance with a $T = 3/2$ isospin 3-neutron force. Phys. Rev. C **93**, 044004 (2016). https://doi.org/10.1103/PhysRevC.93.044004
36. A. Deltuva, R. Lazauskas, Comment on "Is a Trineutron Resonance Lower in Energy than a Tetraneutron Resonance?" Phys. Rev. Lett. **123**, 069201 (2019). https://doi.org/10.1103/PhysRevLett.123.069201
37. K. Kisamori, S. Shimoura, H. Miya, S. Michimasa, S. Ota, M. Assie, H. Baba, T. Baba, D. Beaumel, M. Dozono, T. Fujii, N. Fukuda, S. Go, F. Hammache, E. Ideguchi, N. Inabe, M. Itoh, D. Kameda, S. Kawase, T. Kawabata, M. Kobayashi, Y. Kondo, T. Kubo, Y. Kubota, M. Kurata-Nishimura, C.S. Lee, Y. Maeda, H. Matsubara, K. Miki, T. Nishi, S. Noji, S. Sakaguchi, H. Sakai, Y. Sasamoto, M. Sasano, H. Sato, Y. Shimizu, A. Stolz, H. Suzuki, M. Takaki, H. Takeda, S. Takeuchi, A. Tamii, L. Tang, H. Tokieda, M. Tsumura, T. Uesaka, K. Yako, Y. Yanagisawa, R. Yokoyama, K. Yoshida, Candidate resonant tetraneutron state populated by the ^{4}He(^{8}He,^{8}Be) Reaction. Phys. Rev. Lett. **116**, 052501 (2016). https://doi.org/10.1103/PhysRevLett.116.052501
38. M.S. Hussein, C.L. Lima, M.P. Pato, C.A. Bertulani, Color van der Waals force acting in heavy-ion scattering at low energies. Phys. Rev. Lett. **65**(7), 839 (1990). https://doi.org/10.1103/PhysRevLett.65.839
39. T. Appelquist, W. Fischler, Some remarks on van der Waals forces in QCD. Phys. Lett. B **77**(4-5), 405 (1978). https://doi.org/10.1016/0370-2693(78)90587-7
40. G. Feinberg, J. Sucher, Is there a strong van der Waals force between hadrons? Phys. Rev. D **20**(7), 1717 (1979). https://doi.org/10.1103/PhysRevD.20.1717
41. A.C. Villari, W. Mittig, A. Lépine-Szily, R. Lichtenthäler Filho, G. Auger, L. Bianchi, R. Beunard, J.M. Casandjian, J.L. Ciffre, A. Cunsolo, A. Foti, L. Gaudard, C.L. Lima, E. Plagnol, Y. Schutz, R.H. Siemssen, J.P. Wieleczko, Search for color van der Waals force in ^{208}Pb+^{208}Pb Mott scattering. Phys. Rev. Lett. **71**(16), 2551 (1993). https://doi.org/10.1103/PhysRevLett.71.2551